Vol. 6 No. 2, Dec. 2026

FUAM Journal of Pure and Applied Science

Available online at
www.fuamjpas.org.ng

An official Publication of
College of Science
Joseph Sarwuan Tarka University,
Makurdi.

FUAM Journal of Pure and Applied Science
© College of Science, Joseph Sarwuan Tarka University, Makurdi
https://fuamjpas.org.ng/
Vol.6 No. 2 Dec. 2026

Structure-Dependent Adsorption of Synthetic and Natural Dyes onto Commercial Activated Carbon: Kinetic, Diffusion, and Isotherm Modelling

H.U*. Itodo, M.A. Asema & J.O. Apochi
Department of Chemistry, Joseph Sarwuan Tarka University, Makurdi, P.M.B. 2373 Makurdi, Nigeria
*Correspondence E-mail: itodohu@gmail.com

Received: 27/04/2026 **Accepted**: 12/07/2026 **Published online**: 13/07/2026

Abstract
This study systematically investigates the structure-dependent adsorption of three structurally distinct dyes, Curcumin, Allura red, and Congo red onto commercial activated carbon. Batch adsorption experiments were performed to determine the effects of pH, contact time, initial dye concentration, and adsorbent dosage. The kinetic data obtained were fitted to Pseudo-first-order (PFO), pseudo-second-order (PSO), Elovich, and intraparticle diffusion models, while equilibrium data were studied using Langmuir, Freundlich, Temkin, and linear isotherm models. PSO model best described the adsorption of CUR and CR (R^2 = 0.9994 and 0.9995, respectively), indicating chemisorption-controlled processes, while AR followed PFO kinetics (R^2 = 0.9737), suggesting a predominantly physisorption-driven mechanism. Intraparticle diffusion studies proved that adsorption occurred through a multi-step process involving both boundary layer diffusion and pore diffusion, with diffusion not being the sole rate-limiting step. CUR adsorption conformed to the Langmuir isotherm (R^2 = 0.9972), indicating monolayer adsorption on relatively homogeneous sites. Conversely, AR and CR were better described by the Freundlich model with R^2 = 0.9915 and 0.9960, respectively, reflecting heterogeneous surface adsorption and multilayer formation. Freundlich intensity parameters ($0.91 \leq n \leq 1.31$) and Langmuir separation factors ($0 < R_L < 1$) confirmed favorable adsorption under the conditions investigated. This comparative study demonstrates that the adsorption performance of CAC was strongly influenced by dye molecular structure, with larger and more functionally complex molecules exhibiting stronger surface interactions. Findings provide mechanistic insight into multi-dye adsorption systems and highlight the suitability of CAC in designing targeted removal strategies in wastewater treatment and food processing applications.
Keywords: Dyes, Activated carbon, Adsorption kinetics; Adsorption isotherms, Waste treatment

Introduction

The discharge of synthetic and natural dyes from industrial effluents into our aquatic system poses a significant environmental and health concern due to their persistence, toxicity, and potential carcinogenicity [1, 2]. The global dye market exceeds 1 million tons annually, with approximately 10 – 15% released into water bodies during manufacturing and application processes [3, 4]. Synthetic dyes are of peculiar concern due to their resistance to conventional biodegradation [2, 5] as they reduce light penetration in aquatic ecosystems due their intensive nature, and undergo anaerobic degradation to produce toxic aromatic amines [3, 4].

Among the major array of dyes employed in industries, these three classes of dyes are of utmost important. Congo Red (CR, $C_{32}H_{22}N_6Na_2O_6S_2$, molecular weight: 696.66 g/mol) is a benzidine-based anionic diazo dye widely used in textile industries for cotton, silk, and paper dyeing [4, 6]. Its structure features multiple aromatic rings and sulfonate groups, making it highly water-soluble but resistant to biodegradation [7] and metabolized to benzidine [8].

Allura Red (AR, $C_{18}H_{14}N_2Na_2O_8S_2$, molecular weight: 496.42 g/mol) is a monoazo food dye used extensively in beverages, candies, dairy products, and pharmaceuticals [9, 10]. Although regulatory agencies consider it safe at low concentrations, concerns about potential health effects including hyperactivity in children and possible carcinogenicity have prompted calls for reduced exposure and improved removal [4, 11, 12]. Curcumin (CUR, $C_{21}H_{20}O_6$, molecular weight: 368.38 g/mol) is a natural polyphenolic dye derived from turmeric (*Curcuma longa*). The use of curcumin in food, pharmaceutical, and cosmetic industries is increasing due to its antioxidant, anti-inflammatory, and antimicrobial properties [13, 14]. Curcumin, though generally regarded to be safe, its growing industrial application is of great concern and requires effective removal strategies [15, 16, 17].

Among the various technologies adopted in wastewater treatments, adsorption onto activated carbon remains the most widely used method due to its high surface area, porous structure, versatility, and cost-effectiveness [3, 18]. Commercial activated carbon (CAC) possesses a heterogeneous surface chemistry with various functional

groups such as hydroxyl, carboxyl, and carbonyl that can interact with dye molecules through multiple mechanisms like electrostatic, hydrophobic, π-π stacking, van der Waals forces, and hydrogen bonding interactions [4, 19]. Understanding adsorption mechanism is very important for optimizing dye removal efficiency and designing large-scale treatment systems [8, 20, 21].

Kinetic studies elucidate the rate-controlling steps and potential reaction pathways, while equilibrium isotherm studies provide insights into the surface properties of the adsorbent and the nature of adsorbate-adsorbent interactions [22, 23]. The pseudo-first-order (PFO) model describes adsorption to be proportional to the number of unoccupied sites, which is associated with physisorption [24] while pseudo-second-order (PSO) model assumes chemisorption as the rate-limiting step, involving valence forces through electron sharing or exchange [25]. Both PFO and PSO are the most commonly applied kinetic models [22, 26]. The Elovich model describes chemisorption on heterogeneous surfaces [27, 28], while the intraparticle diffusion model helps identify whether pore diffusion or film diffusion controls the overall adsorption rate [5, 29].

Equilibrium isotherm studies provide insights into surface properties and adsorbate-adsorbent interactions [30, 31]. These models include the Langmuir isotherm which assumes monolayer adsorption onto a homogeneous surface with finite identical sites [32], while the Freundlich isotherm is an empirical model describing reversible adsorption onto heterogeneous surfaces [19, 33]. The Temkin isotherm accounts for adsorbate-adsorbent interactions and assumes a linear decrease in heat of adsorption with surface coverage [34, 35, 36]. While numerous studies have investigated the adsorption of individual dyes onto activated carbon [11, 37], comparative studies examining structurally diverse dyes under identical experimental conditions are limited but are valuable because they explain how molecular structure including molecular size, functional groups, aromaticity, and charge distribution influences adsorption mechanisms [30]. Curcumin (diferuloylmethane) is a hydrophobic polyphenol with β-diketone moiety [13], Allura Red is a small anionic azo dye with sulfonate groups [10, 18], and Congo Red is a larger diazo dye with biphenyl structure and multiple aromatic rings [6, 8, 37].

Therefore, this research aims to: (i) investigate the adsorption kinetics of CR, AR, and CUR, onto CAC fitting kinetic data to PFO, PSO, Elovich, and intraparticle diffusion models; (ii) analyze equilibrium adsorption isotherm models; (iii) determine the best-fitting models for each dye; and (iv) elucidate the underlying adsorption mechanisms. The findings will contribute to a fundamental understanding of dye-activated carbon interactions and inform the selection of appropriate adsorbents for specific dye removal applications.

Materials and Methods

Commercial activated carbon (CAC) of size 0.4 to 0.6 mm was procured from Loba Chemie Pvt. Ltd, Mumbai, India and used without further purification. The three dyes selected as model adsorbates; Congo Red (CR, $C_{32}H_{22}N_6Na_2O_6S_2$), Allura Red (AR, $C_{18}H_{14}N_2Na_2O_8S_2$), and Curcumin E100 (CUR, $C_{21}H_{20}O_6$) were supplied by KEM LIGHT laboratories PVT Ltd. All dyes were of analytical grade (purity >98%) and used without further purification. 1000 mg/L stock solution of each dye was prepared by dissolving 1.0 g of dye in 1 L of distilled water. Working solutions of 10 – 60 mg/L concentrations were obtained by serial dilution. All reagents used in this study were of analytical grade, and distilled water was used throughout the study.

Batch adsorption experiments

All experiments were carried out using 250 mL Erlenmeyer flasks containing 50 mL of dye solution agitated using a mechanical shake (HY-4 Speed adjusting reciprocal vibrator) at room temperature. Each experiment was performed in triplicate, and mean values were reported. Samples were collected at specific intervals, filtered and the absorbance of filtrate was measured using a SUR GISPIC spectrophotometer (Model No SM7525 UV) at the respective λmax for each dye.

Kinetic studies

For kinetic experiments, 0.5 g of CAC was added to 50 mL of dye solution at initial concentration 50 mg/L. Flasks were agitated, and aliquots were withdrawn at predetermined time intervals (0, 30, 60, 90, 120, 150, and 180 min). Samples were immediately centrifuged at 2000 rpm using for 10 min to separate adsorbent particles Centurion scientific Centrifuge, model K241 series, UK., and supernatant dye concentrations were analysed.

The adsorption capacity and removal efficiency at time t, RE (%), were calculated using:

$$q_t = \frac{(C_o - C_t)V}{W} \qquad (1)$$

$$RE\ (\%) = \frac{C_o - C_t}{C_o} \times 100 \qquad (2)$$

where q_t and RE are adsorption capacity and removal efficiency at time t, C_0 and C_t (mg/L) are initial and time t concentrations, V (L) is volume of the solution, and W (g) is adsorbent mass.

Equilibrium isotherm studies

For isotherm studies, varying initial dye concentrations (10 – 60 mg/L) were contacted with fixed CAC dose (0.5 g/50 mL) and agitated for 120 min to ensure equilibrium. Samples were processed as described for kinetic studies, and equilibrium concentration C_e (mg/L) was measured. The amount adsorbed at equilibrium, qe (mg/g), was calculated as:

$$q_e = \frac{(C_o - C_e)V}{W} \qquad (3)$$

where C_0 and C_e (mg/L) are initial and equilibrium concentrations, V (L) is volume of the solution, and W (g) is adsorbent mass.

Effect of Operational Parameters

Effect of initial concentration on removal efficiency

The effect of initial dye concentration on removal efficiency was examined by varying concentration from (10 – 60 mg/L) while maintaining constant adsorbent dosage (0.5 g), pH (7), and room temperature.

Effect of adsorbent dosage

The effect of adsorbent mass on removal efficiency was investigated by varying CAC dosage (0.5 – 3.0 g) in 50 mL of dye solution at fixed initial concentration 50 mg/L, kept

in separate flasks and allowed to interact for 120 min contact time using a mechanical shaker. Each mixture was filtered, the filtrate absorbance of was taken at the respective λmax for each dye.

Effect of contact time on removal efficiency

The effect of contact time on dye removal efficiency was investigated and to determine equilibrium time, adsorption experiments were conducted over varying contact times (30 – 180 min). Samples were collected at specific intervals, filtered and the absorbance of filtrate was taken at the respective λmax for each dye.

Effect of initial pH

The effect of solution pH on removal efficiency was studied by adjusting initial pH (3 – 11) using 0.1 M HCl/NaOH solutions. Experiments were conducted at fixed initial concentration (50 mg/L), adsorbent dosage (0.5 g/50 mL), and contact time (120 min). Final pH was not controlled to simulate realistic wastewater treatment conditions where pH may drift during adsorption.

Adsorption kinetic modeling

Four kinetic models were applied to study experimental data obtained.

Pseudo-first-order (PFO) kinetic model [24]

The linear equation form for Pseudo-first kinetic model is given as;

$$\log(q_e - q_t) = logq_e - \left({}^{k_1}/_{2.303}\right)t \quad (4)$$

Where; q_e and q_t are sorption capacities at equilibrium and at any time, t in mg/g. k_1 is the Pseudo-first order rate constant in g/mg.min^{-1}. The value for k_1 and log q_e can be obtain from the slope and intercept of the graph by plotting $\log(q_e - q_t)$ against t.

Pseudo-second-order (PSO) model [25]

$$\frac{t}{q_t} = \frac{1}{k_2 q_e^2} + \frac{1}{q_e}t \quad (5)$$

where k_2 (g/mg·min) is the PSO rate constant. A plot of t/qt against t gives slope 1/qe and intercept $\frac{1}{k_2 q_e^2}$.

Elovich model [27]

$$q_t = \frac{1}{\beta}ln(\alpha\beta) + \frac{1}{\beta}ln(t) \quad (6)$$

Where α (mg/g·min) is initial adsorption rate and β (g/mg) is desorption constant. A plot of qt versus ln(t) yields slope 1/β and intercept (1/β) ln(αβ).

Intraparticle diffusion model [29, 38]

$$q_t = k_{id}t^{1/2} + C \quad (7)$$

Where k_{id} (mg/g·min$^{1/2}$) is intraparticle diffusion rate constant and C (mg/g) is intercept related to boundary layer thickness. If the plot passes through origin (C = 0), intraparticle diffusion is the sole rate-controlling step.

Equilibrium isotherm modeling

Four isotherm models were employed to analyze the equilibrium data obtained in this study:

Langmuir Isotherm [5, 32]

The linear form of Langmuir equation can be represented as;

$$\frac{1}{q_e} = \frac{1}{q_m} + \frac{1}{q_m C_e K_L} \quad (8)$$

Where q_e = amount of dye adsorbed per gram of the adsorbent at equilibrium (mg/g), q_m = maximum monolayer coverage capacity (mg/g), C_e = equilibrium concentration of adsorbate (mg/L) and K_L = Langmuir isotherm constant (L/mg)

The essential features of the Langmuir isotherm R_L, which is a dimensionless constant referred to as separation factor or equilibrium parameter is given as;

$$R_L = \frac{1}{1+(1+K_L C_0)} \quad (9)$$

R_L value indicates the adsorption nature to be either unfavourable if R_L>1, linear if R_L =1, favorable if 0< R_L<1 and irreversible if R_L= 0.

Freundlich isotherm [33]

The linearized form of Freundlich model is expressed as:

$$\log q_e = \log K_f + \frac{1}{n}\log c_e \quad (10)$$

Where q_e = amount of dye adsorbed per gram of the adsorbent at equilibrium (mg/g), C_e = equilibrium concentration of adsorbate (mg/L), K_f = Freundlich isotherm constant (mg/g) and n = adsorption intensity. The value of n indicates: n > 1 favorable adsorption, n = 1 linear adsorption, and n < 1 cooperative adsorption.

Temkin isotherm [34, 35]

$$q_e = BlnK_T + BlnC_e \quad (11)$$

where B = RT/b_T (J/mol) is related to Temkin heat of adsorption, K_T (L/g) is Temkin isotherm equilibrium binding constant, R (8.314 J/mol·K) is universal gas constant, T (K) is absolute temperature, and b_T is the Temkin isotherm constant linked to the energy parameter, B.

Linear isotherm [30]

$$q_e = K_d C_e + C \quad (12)$$

where K_d (L/g) is distribution coefficient. This model assumes linear relationship between adsorbed and equilibrium concentrations, typically applicable at low concentrations or for partition-dominated mechanisms.

Statistical analysis

All experiments were conducted in triplicate, and mean values were reported. Model fitting was evaluated using correlation coefficient (R^2) and the model with R^2 closest to unity was considered best-fitting. Model selection considered both statistical fit and mechanistic plausibility.

Results and Discussion

Parametric studies

Effect of initial concentration on removal efficiency

The effect of initial concentration (10 – 60 mg/L) on removal efficiency at equilibrium is presented in Figure 1. Congo Red (CR) exhibited minimal concentration dependence, with removal decreasing only from approximately 95% at 10 mg/L to 80% at 60 mg/L showing a 15% reduction. The shallow decline reflects CR's high affinity and cooperative mechanism [21]. At low concentrations, the ratio of available sites to dye molecules is high, enabling near-complete removal. As concentration increases, the cooperative effect (n < 1) compensates for reduced site availability, maintaining high removal even at elevated concentrations [7, 39]. This behaviour is ideal for treating variable-strength wastewater without extensive dilution or pH adjustment [6].

Allura Red (AR) showed steady concentration-dependent decline, with removal decreasing from approximately 45% at 10 mg/L to 20% at 60 mg/L presenting a 55% relative reduction. The steady decline reflects AR's weak binding and absence of cooperative effects [9, 10]. At low concentrations, AR accesses the most favourable sites, achieving moderate removal. As concentration increases, competition for limited favourable sites increases, and the weak binding energy results in lower overall removal [20]. This behaviour limits AR's practical treatability using unmodified CAC [4].

Curcumin (CUR) exhibited moderate concentration dependence, with removal decreasing from approximately 80% at 10 mg/L to 50% at 60 mg/L giving a 37.5% reduction. The decline reflects monolayer saturation behaviour consistent with Langmuir isotherm [32]. At low concentrations, sufficient homogeneous sites are available for CUR to bind via hydrogen bonding. As concentration increases, the finite number of sites becomes saturated, leading to decreased removal [19, 23]. CUR lacks cooperative effects unlike CR, so once the monolayer is complete, additional molecules cannot be accommodated [14, 40].

Effect of adsorbent dosage on removal efficiency

The effect of CAC dosage (0.5 – 3.0 g/50 mL) on removal efficiency at C_0 = 50 mg/L is presented in Figure 2. Congo Red (CR) showed minimal dosage dependence, with removal decreasing only slightly from 85% at 0.5 g to 81% at 2.5 – 3.0 g. The consistently high removal across dosages confirms CR's strong binding and efficient site utilization [41]. Even at the lowest dosage, CR achieves 85% removal, indicating that cooperative effects enable high surface coverage with minimal adsorbent [8]. The slight decrease at higher dosages may reflect particle aggregation reducing effective surface area [3].

Allura Red (AR) exhibited dramatic dosage-dependent decline, with removal dropping from 33% at 0.5 g to only 3% at 3.0 g, about 80% relative decrease. This striking decline is the strongest evidence for extremely weak binding which may be an indication of desorption. Typically, increasing adsorbent dosage increases removal by providing more sites but desorption sets in when sites are occupied. The observed decrease suggests that at higher carbon dosages, AR exhibits reverse adsorption [21]. Possible explanations include: (i) Release of soluble impurities from carbon at higher solid: liquid ratios that compete with AR [3, 42], (ii) pH shifts with increasing carbon dosage that move the system away from optimal conditions for electrostatic attraction [19], and (iii) aggregation of carbon particles trapping AR in solution rather than allowing access to interior pores [36]. The plateau at 3% at higher dosages may represent baseline adsorption onto the small fraction of high-energy sites that can bind AR irreversibly [31].

Curcumin (CUR) showed steady dosage-dependent decline, with removal decreasing from 53% at 0.5 g to 32% at 3.0 g, about 38% reduction. The decreasing removal with increasing dosage is contrary to one's intuitive expectation but consistent with monolayer adsorption [32]. At fixed dye concentration, once all dye is adsorbed (occurring more completely at lower adsorbent: dye ratios), additional adsorbent cannot increase removal because no more dye is available [16]. The decline may also reflect CUR's complex kinetic behaviour, where higher carbon dosages aggravate the rearrangement phenomena observed in time studies [13].

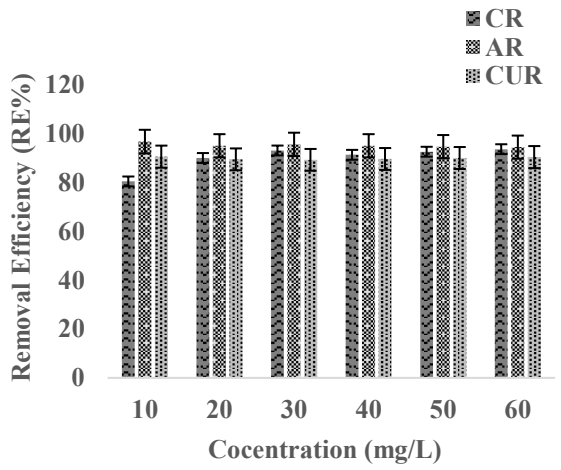

Figure 1 : Effect of Initial concentration on Removal Efficiency of CR, AR and CUR Uptake onto Commercial Activated Carbon

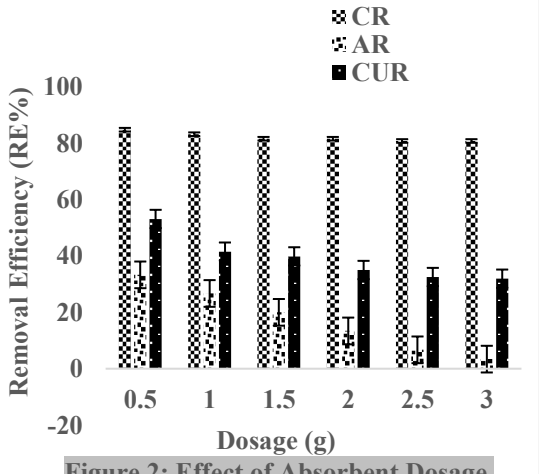

Figure 2: Effect of Absorbent Dosage on Removal Efficiency of CR, AR and CUR Uptake onto Commercial Activated Carbon

Effect of contact time on removal efficiency

The time-dependent removal efficiency (30 – 180 min) for each dye at C_0 = 50 mg/L, dosage = 0.5 g/50 mL is presented in Figure 3. Congo Red (CR) demonstrated exceptionally rapid adsorption, achieving 93% removal within 30 min, the highest among all dyes at any given time. Removal remained consistently high throughout, decreasing only marginally to 88% at 180 min (5% reduction over 150 min). The rapid attainment of >90% removal confirms the high affinity predicted by PSO

kinetics and cooperative mechanism [28]. The slight decrease over time may reflect equilibrium rebalancing as the system approaches true thermodynamic equilibrium, or minor experimental variation at high removal levels where small absolute changes produce noticeable percentage differences [43]. The sustained high removal confirms that CR remains strongly bound once adsorbed, consistent with chemisorption [8]. The time profile supports the cooperative mechanism as initial rapid uptake via strong interactions (electrostatic, π-π) creates a favourable surface for continued adsorption, maintaining high removal throughout [41].

Allura Red (AR) exhibited slow, steady increase in removal from 28% at 30 min to 43% at 180 min, a 15% rise over 150 min with no plateau reached by 180 min. This gradual increase is characteristic of intraparticle diffusion-controlled physisorption [29, 36]. The absence of rapid initial uptake distinguishes AR from CR and CUR dyes confirming weak physical forces, rather than specific chemical interactions, driven adsorption [44]. The lack of plateau by 180 min suggests that equilibrium requires longer contact times, consistent with slow pore diffusion kinetics [45]. The time profile aligns perfectly with PFO kinetics and near-zero intraparticle intercept, making pore diffusion the dominant rate-controlling mechanism [36].

Curcumin (CUR) presented the most complex time-dependent profile in the order; 62% at 30 min to 79% at 60 min (increase) to 42% at 90 min (sharp decline) to 51–52% at 150 – 180 min (partial recovery). This unusual pattern reflects the complexity of CUR adsorption and can be explained by:

Stage 1: the 0 – 60 min rapid initial adsorption of 62% to 79% corresponds to the occupation of available surface sites via hydrogen bonding, which is consistent with PSO kinetics [16].

Stage 2: the 60 – 90 min apparent desorption of 79% to 42% which may result from molecular rearrangement since CUR exists in keto-enol tautomeric equilibrium and upon initial adsorption, molecular reorientation may temporarily release some molecules as the system seeks the most energetically favourable configuration possible [13]. Surface diffusion also play a role as adsorbed molecules may move to more favourable sites, causing temporary desorption of loosely bound molecules before stable binding [46]. Finally, CUR is known to degrade in aqueous media, especially under light and as a result, degradation products might compete for sites or complex with CUR in solution leading to its instability [47].

Stage 3: the 90 – 180 min re-equilibration from 42% to 52% may represents stabilization as molecules find stable binding configurations. The final removal (52%) is lower than the initial peak (79%), suggesting that the thermodynamically favoured equilibrium coverage is lower than the kinetic driven initial uptake, a phenomenon observed in some adsorption systems [48]. Despite this complexity, the overall profile is consistent with PSO kinetics when considered over the entire time period, as the PSO model accommodates changes in adsorption rate with surface coverage [33].

Effect of pH on removal efficiency

The effect of initial pH (3 – 11) on removal efficiency at C_0 = 50 mg/L, dosage = 0.5 g/50 mL, contact time = 120 min is presented in Figure 4. Congo Red (CR) exhibited moderate pH dependence, with removal efficiency decreasing gradually from 89% at pH 3 to 80% at pH 11 (9% reduction). The steady high removal efficiency across all pH values indicates that CR utilizes multiple binding modes [1] because at low pH of 3 to 5, electrostatic attraction between anionic -SO_3^- and positively charged carbon surface dominates, contributing to highest removal efficiency [15] while at neutral to alkaline pH of 7 to 11, the surface becomes negatively charged, thereby diminishing electrostatic attraction, but π-π stacking, hydrophobic interactions, and hydrogen bonding maintain high removal [39]. The moderate pH dependence confirms that non-electrostatic forces are significant for CR, consistent with cooperative mechanism [30].

Allura Red (AR) showed strong pH dependence, with removal efficiency decreasing from 90% at pH 3 to 72% at pH 11 (18% reduction). The strong pH dependence indicates that electrostatic attraction is the primary binding mechanism for AR [44]. The sharp decline between pH 5 – 7 identifies the approximate pH of the CAC as 6 to 7, consistent with literature [3]. The dramatic pH sensitivity AR confirms its reliance on weak electrostatic forces without significant secondary binding modes [10].

Curcumin (CUR) exhibited minimal pH dependence, with removal decreasing only slightly from 58% at pH 3 to 52% at pH 11 (6% reduction). The minimal pH dependence indicates that hydrogen bonding and π-π interactions, rather than electrostatics, drive CUR adsorption [13] because phenolic -OH groups which are relatively insensitive to pH, form hydrogen bonds with carbon surface oxygen groups [14] while the aromatic rings (pH-independent) participate in π-π interactions with graphitic planes [49]. The slightly higher removal at acidic pH may reflect greater molecular stability of CUR at low pH rather than enhanced electrostatic attraction, as CUR degrades more rapidly under alkaline conditions [47].

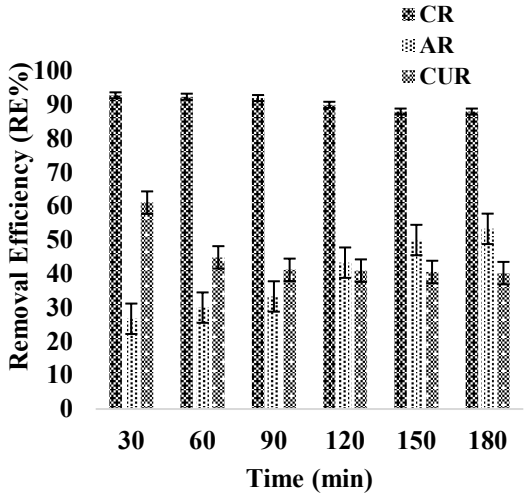

Figure 3: Effect of Contact Time on Removal Efficiency of CR, AR and CUR Uptake onto Commercial Activated Carbon

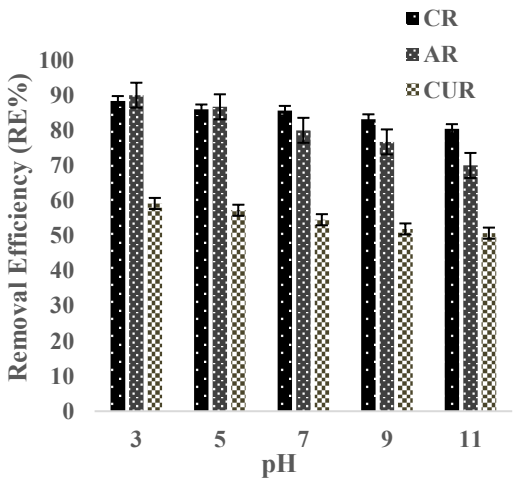

Figure 4: Effect of pH on Removal Efficiency of CR, AR and CUR Uptake onto Commercial Activated Carbon

Adsorption kinetic studies

The kinetic parameters for the adsorption of CR, CUR, and AR onto commercial activated carbon were determined by fitting experimental data to the PFO, PSO, Elovich, and intraparticle diffusion models. The linear plots are presented in Figures 5 – 8, and the calculated parameters along with correlation coefficients are summarized in Table 1.

Pseudo-first-order model

The PFO model plots of log (qe - qt) versus t (Figure 5) exhibited varying degrees of linearity for the three dyes. As presented in Table 1, CUR showed a poor fit to the PFO model with R^2 = 0.6245, indicating that the adsorption of CUR does not follow first-order kinetics. The negative slope (-0.0314) and the discrepancy between calculated and experimental qe values further confirm the inapplicability of this model for CUR. In contrast, AR demonstrated good correlation with the PFO model (R^2 = 0.9737), suggesting that physical adsorption processes may govern its initial uptake. The positive slope (0.0691) is notable since in ideal PFO kinetics, the slope should be negative. This anomaly may indicate experimental errors or possible desorption phenomena during the initial phase, warranting cautious interpretation. CR exhibited moderate fit to the PFO model (R^2 = 0.9173), though other models provided superior description of its kinetic behaviour.

Pseudo-second-order model

The PSO model plots of t/qt versus t (Figure 6) revealed striking differences among the three dyes. CUR and CR exhibited exceptional linearity with R^2 values of 0.9994 and 0.9995, respectively (Table 1). These near-unity correlation coefficients strongly indicate that the adsorption of both dyes follows PSO kinetics, implying that chemisorption involving valence forces through electron sharing or exchange between the adsorbent and adsorbate is the rate-limiting step [36]. The excellent fit of the PSO model for CUR suggests that its β-diketone moiety and phenolic hydroxyl groups may form specific chemical interactions (hydrogen bonding or complexation) with oxygen-containing functional groups on the CAC surface [22, 26]. Similarly, the PSO fit for CR indicates strong chemical interactions, likely involving the multiple aromatic rings and sulfonate groups of the dye with the carbon surface [7,39]. For AR, the PSO model yielded a moderate R^2 of 0.8956. More importantly, the intercept value (1062.2) is anomalously high, which may be as a result of concentration error. This confirms that despite the moderate correlation, the PSO model is inappropriate for describing AR adsorption.

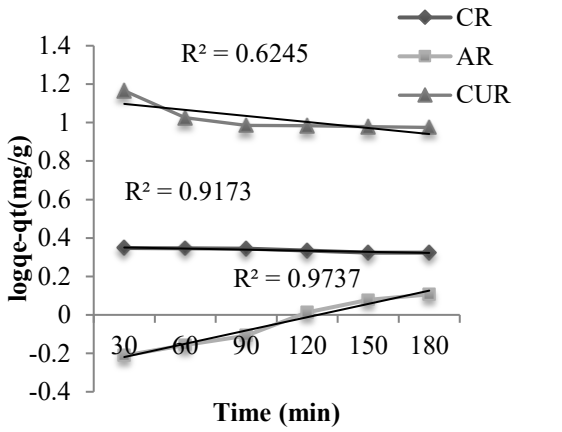

Figure 5: Pseudo-first Order Kinetics Plot for CR, AR and CUR Uptake onto Commercial Activated Carbon

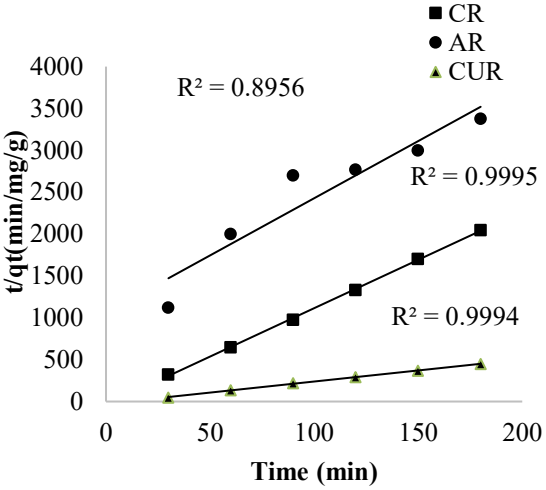

Figure 6: Pseudo-Second Order Kinetics Plot for CR, AR and CUR Uptake onto Commercial Activated Carbon

Elovich model

The Elovich kinetic model, which describes chemisorption on heterogeneous surfaces [27], showed poor correlation for CUR (R^2 = 0.5943) but good correlation for AR (R^2 = 0.9688) and CR (R^2 = 0.9187) (Table 1). The good fit for AR suggests that its adsorption may involve heterogeneous surface sites [10], consistent with the Freundlich isotherm findings [11]. For CR, the moderate Elovich fit (R^2 = 0.9187) combined with the excellent PSO fit (R^2 = 0.9995) suggests that while surface heterogeneity exists, the overall rate is controlled by chemical bonding rather than surface diffusion [37, 49].

Intraparticle diffusion model

The intraparticle diffusion model provides insights into the rate-controlling steps of adsorption processes. According to Weber and Morris [29], if intraparticle diffusion is the sole rate-limiting step, the plot of qt versus $t^{0.5}$ should be linear and pass through the origin. Multi-linearity indicates that multiple processes influence adsorption processes. As shown in Figure 8, none of the dyes exhibited intercepts of zero, indicating that intraparticle diffusion is not the only rate-controlling mechanism [38]. CUR showed poor linearity (R^2 = 0.7062) with a relatively high intercept (0.6778), suggesting significant boundary layer control. CR exhibited moderate linearity (R^2 = 0.8728) with an intercept of 0.0974, indicating some boundary layer effects but less pronounced compared to CUR while AR demonstrated good linearity (R^2 = 0.9334) with an intercept very close to zero (0.0037). This near-zero intercept suggests that intraparticle diffusion may be the dominant rate-controlling mechanism for AR, consistent with its physisorption behaviour [20].

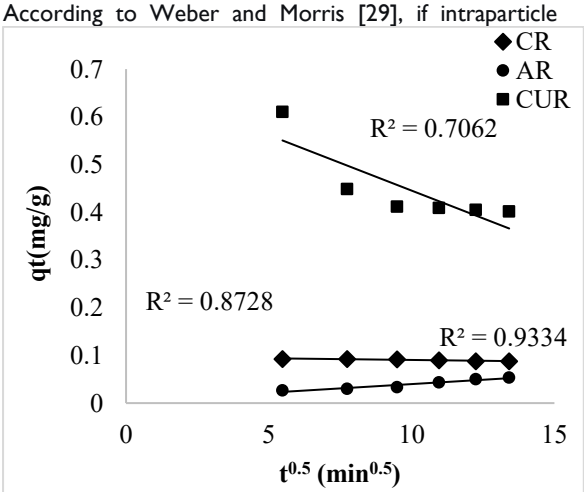

Figure 7: Intra-particle Diffusion Plot for Congo Red (CR), Allura Red (AR) and Curcumin (CUR) Uptake onto Commercial Activated Carbon

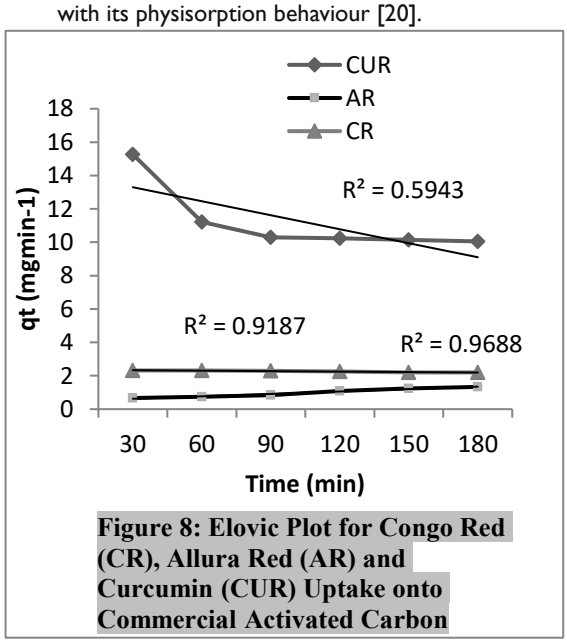

Figure 8: Elovic Plot for Congo Red (CR), Allura Red (AR) and Curcumin (CUR) Uptake onto Commercial Activated Carbon

Table 1: Kinetic Parameters for CR, AR and CUR Dye Adsorption onto CAC

Kinetic Models	Parameters	CR	AR	CUR
Pseudo-first order	Slope	-0.0056	0.0691	-0.0314
	Intercept	0.3561	-0.2885	1.1288
	R^2	0.9173	0.9737	0.6245
Pseudo-second order	Slope	11.554	13.654	2.6442
	Intercept	-40.785	1062.2	-25.579
	R^2	0.9995	0.8956	0.9994
Elovich	Slope	-0.028	0.145	-0.839
	Intercept	2.3613	0.4783	-0.028
	R^2	0.9187	0.9688	0.5943
Intra-particle diffusion	Slope	-0.0007	0.0036	-0.0232
	Intercept	0.0974	0.0037	0.6778
	R^2	0.8728	0.9334	0.7062

Adsorption isotherms

Equilibrium adsorption data obtained were subjected Langmuir, Freundlich, Temkin, and linear isotherm models. The calculated parameters and correlation coefficients are presented in Table 2.

Langmuir isotherm

The Langmuir model assumes monolayer adsorption onto a homogeneous surface with finite identical sites [36]. Among the three dyes, CUR exhibited the best fit to the Langmuir model with R^2 = 0.9972 (Table 2), indicating that CUR forms a monolayer on the activated carbon surface [40]. This finding aligns with the PSO kinetic result, collectively suggesting that CUR adsorbs via specific chemical interactions onto uniform binding sites. The maximum adsorption capacity (q_m) for CUR, calculated from the Langmuir slope ($1/q_m$ = slope), was approximately 0.08 mg/g (based on slope = 12.539). This value appears too low, possibly due to the concentration range studied in this work. CR showed good fit to the Langmuir model with R^2 = 0.9688, but shows extremely high slope (5898.3) and large negative intercept (-60.743) which may be due to numerical instability in the linear regression. AR exhibited good correlation with the Langmuir model (R^2 = 0.9716), but as will be discussed, the Freundlich model provided superior fit.

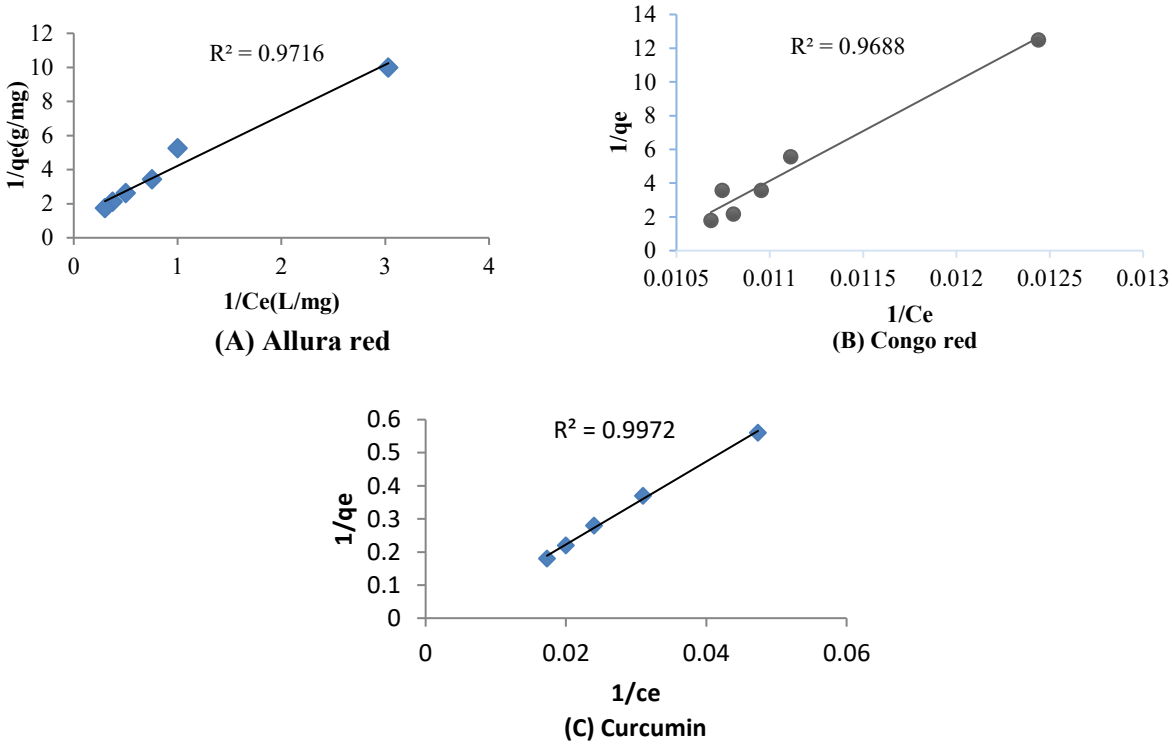

Figure 9: Langmuir Adsorption Isotherm Plot for (A) Allura Red, (B) Congo Red, and (C) Curcumin Uptake onto Commercial Activated Carbon (CAC)

Freundlich isotherm

The Freundlich model, which describes adsorption onto heterogeneous surfaces [33], provided excellent fits for AR (R^2 = 0.9915) and CR (R^2 = 0.9960). CUR also showed excellent fit to the Freundlich model (R^2 = 0.9955), but the Langmuir fit was marginally better (0.9972 versus 0.9955), supporting monolayer adsorption as the primary mechanism. The Freundlich exponent n provides valuable information about adsorption favourability and mechanisms. For AR, 1/n = 0.7655, yielding n = 1.31. Since

n > 1, this indicates favourable adsorption onto a heterogeneous surface [30]. The value of 1.31 suggests moderate heterogeneity, with adsorption intensity decreasing as surface coverage increases. For CR, 1/n = 1.0987, yielding n = 0.91. The condition n < 1 is particularly interesting and indicates cooperative adsorption [31]. This means that adsorbed CR molecules facilitate the adsorption of additional molecules, possibly through dye-dye interactions such as π-π stacking between aromatic rings or aggregation phenomena. CR is known to form aggregates in solution and on surfaces due to its planar structure and extended conjugation [32]. This cooperative effect explains why CR, despite following PSO kinetics (indicating chemisorption), conforms to the Freundlich rather than Langmuir isotherm. For CUR, 1/n = 1.0977, yielding n = 0.91 as well, identical to CR. However, given the superior Langmuir fit, the apparent n < 1 for CUR may reflect the limited concentration range studied rather than true cooperative adsorption.

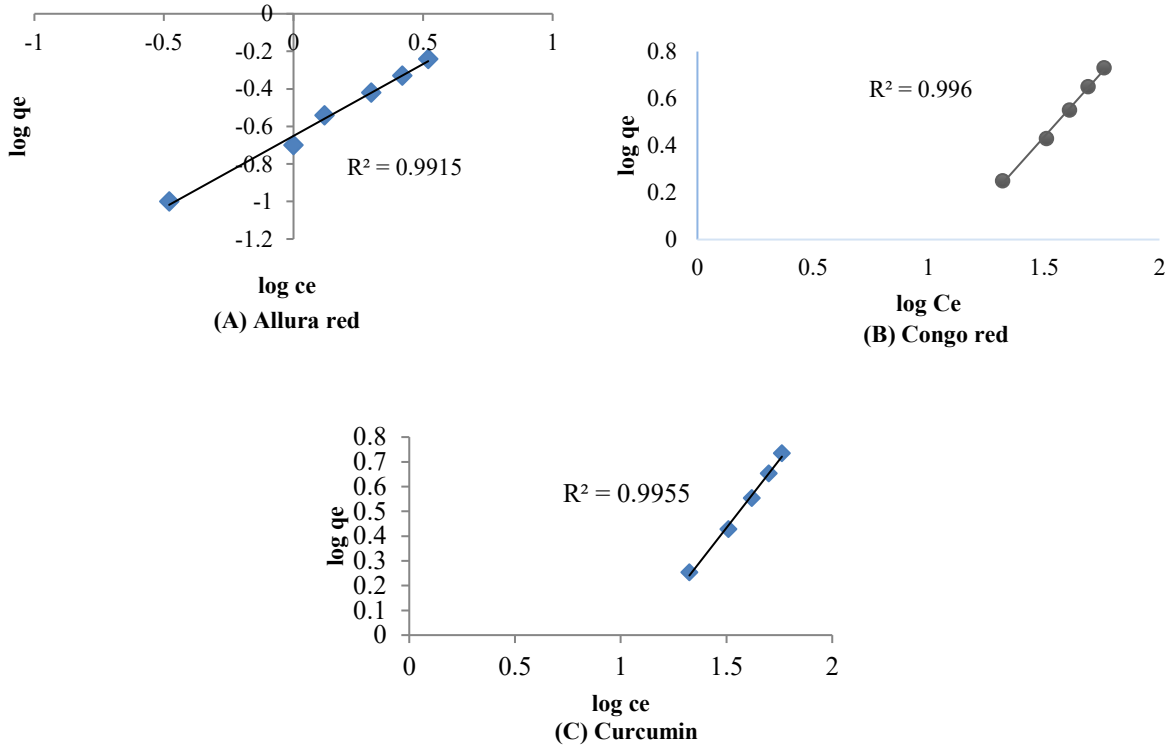

Figure 10: Freundlich Adsorption Isotherm Plot for (A) Allura Red, (B) Congo Red, and (C) Curcumin Uptake onto Commercial Activated Carbon (CAC)

Temkin isotherm

The Temkin model assumes that, the heat of adsorption decreases linearly with surface coverage due to adsorbate-adsorbate interactions, rather than being constant (Langmuir) or logarithmic (Freundlich) [35]. It shows moderate fits for all dyes with R^2 ranging from 0.9047 to 0.949. Temkin analysis complements the linear isotherm model by revealing how adsorption energetics change with coverage, offering a more nuanced understanding of dye–adsorbent interactions on CAC.

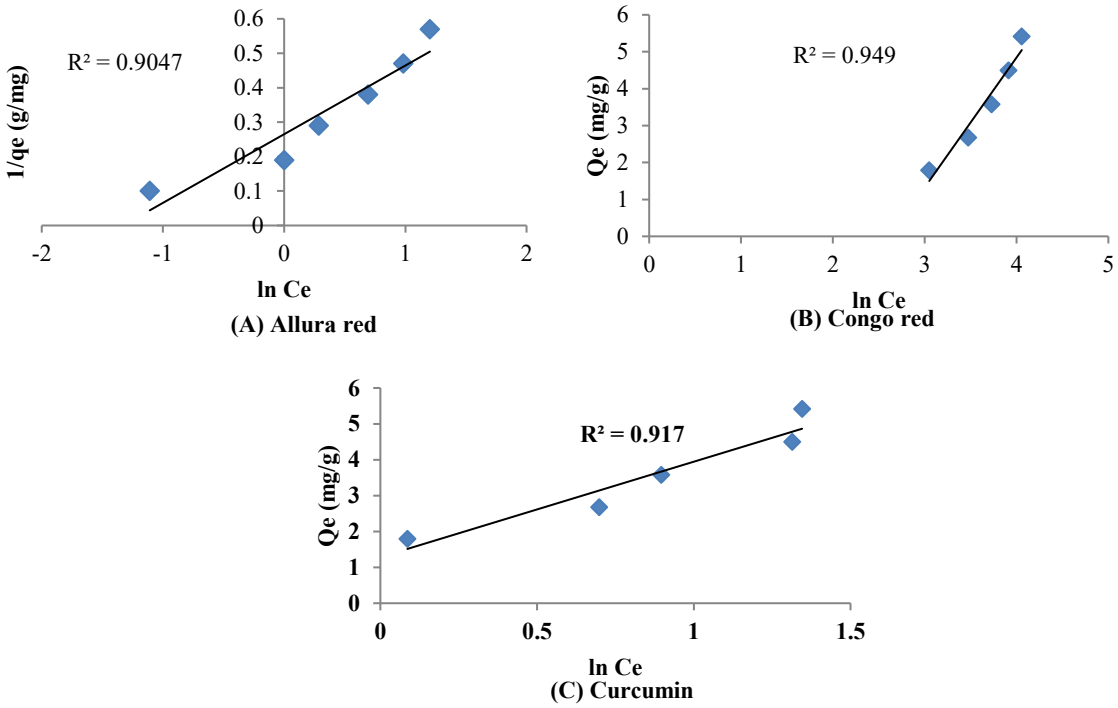

Figure 11: Temkin Adsorption Isotherm Plot for (A) Allura Red, (B) Congo Red, and (C) Curcumin Uptake onto Commercial Activated Carbon (CAC)

Linear isotherm

The linear isotherm model, representing partition-controlled adsorption at low concentrations [20], exhibited excellent fits for AR, R^2 = 0.9908 and CR, R^2 = 0.9936. The linear fit for AR, R^2 = 0.9908 is comparable to its Freundlich fit (0.9915), suggesting that at the concentrations studied, AR adsorption may operate in the linear region of the Freundlich isotherm, corresponding to low surface coverage.

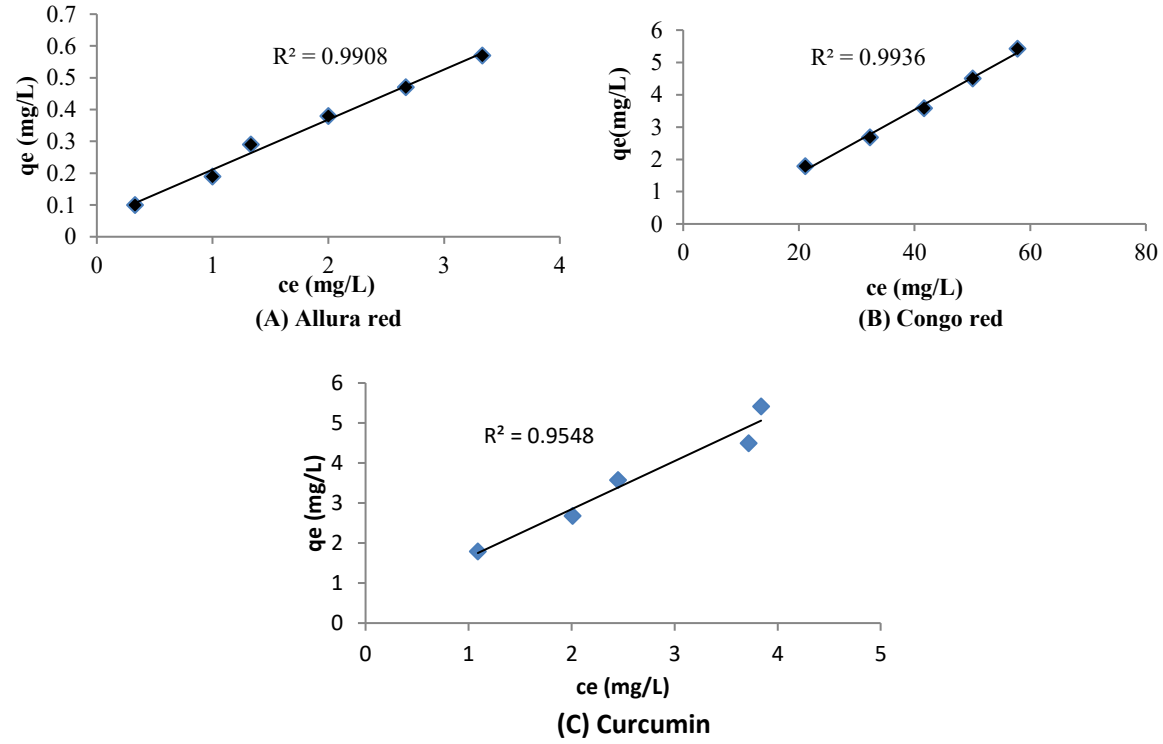

Figure 12: Linear Adsorption Isotherm Plot for (A) Allura Red, (B) Congo Red, and (C) Curcumin Uptake onto Commercial Activated Carbon (CAC)

Table 2: Isotherm Parameters for CR, AR and CUR Dye Adsorption onto CAC

Isotherms	Parameters	CR	AR	CUR
Linear	K_d (L/g)	0.0990	0.1573	1.2029
	Intercept	-0.4226	0.0539	0.4399
	R^2	0.9936	0.9908	0.9548
Freundlich	1/n	1.0987	0.7655	0.3456
	n	0.9102	1.3063	2.8935
	K_f	0.0614	0.2236	1.5778
	R^2	0.9960	0.9915	0.9955
Langmuir	Q_m(mg/g)	-	0.7970	-
	K_L(L/g)	-	0.4230	-
	Slope	5898.3	2.9665	12.539
	R^2	0.9688	0.9716	0.9972
Temkin	B_T (mg/g)	3.5173	0.1994	2.6612
	A_T (L/mg)	0.073	3.78	1.62
	R^2	0.949	0.9047	0.917

Mechanistic interpretation

Integrating the kinetic and isotherm findings reveals three distinct adsorption mechanisms for the three dyes studied.

Congo red (cooperative chemisorption)

CR adsorption follows PSO kinetics with $R^2 = 0.9995$, but conforms to the Freundlich isotherm with $R^2 = 0.9960$, and $n < 1$. This combination indicates chemisorption with cooperative effects [33, 50]. CR is a large, planar, diazo dye with multiple aromatic rings and sulfonate groups [4]. The PSO kinetics suggests that the initial attachment involves chemical bonding, likely through electrostatic interactions between sulfonate groups and positively charged carbon surface sites or through hydrogen bonding [21]. However, the Freundlich fit with $n < 1$ indicates that once initial molecules adsorb, they modify the surface to facilitate further adsorption [33]. This cooperative behaviour is attributed to π-π stacking between the aromatic backbones of adsorbed [21] and free CR molecules, hydrophobic interactions driving aggregation of the dye on the carbon surface, and Van der Waals forces between adjacent dye molecules [7]. This phenomenon, which is sometimes called "sorbent-assisted sorption" or "dye aggregation on surfaces," has been reported for other planar aromatic dyes [41]. The moderate intercept in the intraparticle model (0.0974) suggests less boundary layer resistance compared to CUR, possibly due to the strong driving force from cooperative effects [21].

Allura red (physisorption on heterogeneous surface)

AR adsorption is best described by PFO kinetics with $R^2 = 0.9737$, and the Freundlich isotherm with $R^2 = 0.9915$, and $n = 1.31$ (>1). This combination indicates favorable physisorption onto a heterogeneous surface [22]. AR is a smaller, monoazo dye with sulfonate groups [10]. The PFO kinetics suggest that the adsorption rate is proportional to the number of unoccupied sites, typical of physical adsorption processes involving weak van der Waals forces, hydrophobic interactions, or hydrogen bonding [19]. The Freundlich fit with $n > 1$ indicates favourable adsorption onto energetically heterogeneous sites, with adsorption intensity decreasing as the strongest sites are progressively occupied [30]. The near-zero intercept in the intraparticle diffusion model (0.0037) strongly suggests that intraparticle diffusion is the dominant rate-controlling mechanism, consistent with physisorption where pore diffusion often governs the overall rate [29, 36].

Curcumin (monolayer chemisorption)

CUR adsorption is best described by PSO kinetics with $R^2 = 0.9994$, and the Langmuir isotherm with $R^2 = 0.9972$. This combination shows monolayer chemisorption onto a homogeneous surface [25]. CUR (diferuloylmethane) contains two methoxyphenol groups connected by a β-diketone moiety, its enol form can form strong hydrogen bonds with oxygen-containing functional groups (carboxyl, hydroxyl) on activated carbon surfaces [14, 16]. Also, the aromatic rings may participate in π-π interactions with the graphitic planes of carbon [15]. These specific interactions occur at finite, energetically equivalent sites, leading to monolayer coverage [38]. The relatively high intercept in the intraparticle diffusion model (0.6778) suggests that film diffusion significantly influences the overall rate, consistent with chemisorption where surface reaction rather than pore diffusion is rate-limiting [14].

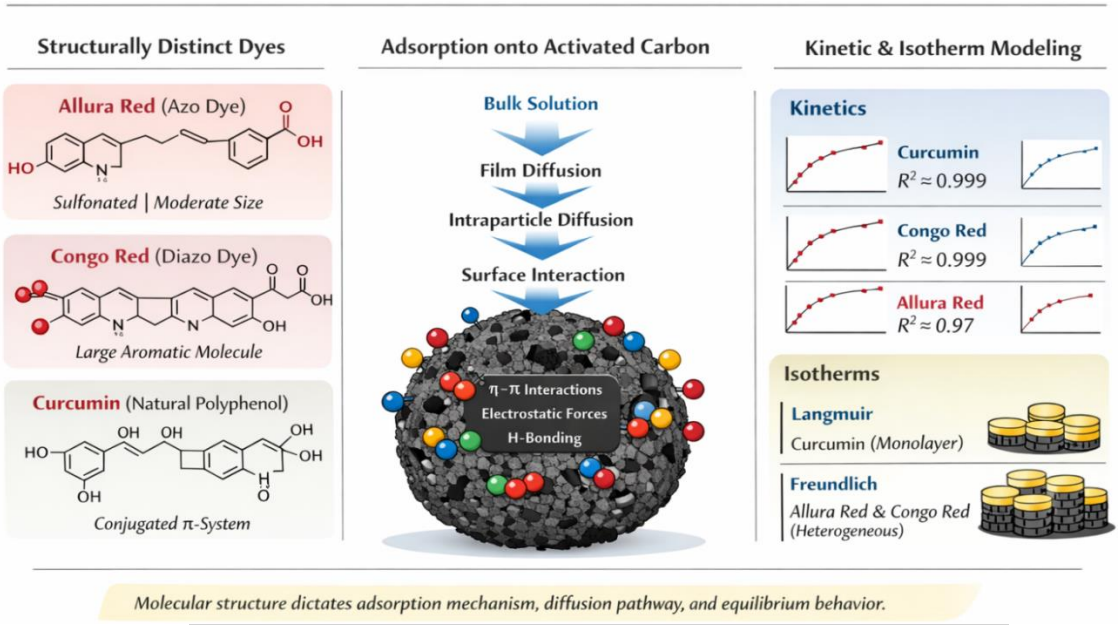

Plate 1: Structural-Dependent of CR, AR and CUR Adsorption onto CAC

Comparison with literature

The findings from this study align with and extend previous research on dye adsorption onto carbonaceous materials. The combination of PSO kinetics and Freundlich isotherm with n < 1 has been reported by Dawood and Sen [41] for adsorption of CR onto pine cone-derived activated carbon, attributing the cooperative effect of CR molecules on the carbon surface to its aggregation tendency. Purkait et al. [6] also observed Freundlich behaviour for CR adsorption on activated carbon and noted the importance of π-π interactions in the adsorption mechanism. AR adsorption studies are comparatively limited. However, Erdem et al. [10] reported PFO kinetics for AR adsorption onto magnetic nanoparticles, consistent with our findings. The Freundlich isotherm for azo dye adsorption onto activated carbon is well-documented, with n values between 1 and 2 commonly reported [28]. Several studies have reported PSO kinetics for CUR adsorption onto various adsorbents. Gholami et al. [14] observed PSO kinetics for CUR adsorption onto functionalized multi-walled carbon nanotubes, attributing this to chemical interactions between its β-diketone group and surface functional groups. Similarly, Chatterjee et al. [16] reported Langmuir isotherm behavior for CUR adsorption onto chitosan hydrogels, consistent with monolayer chemisorption.

Implications for wastewater treatment

The distinct adsorption mechanisms observed in this study have practical implications for wastewater treatment design as presented on Table 3.

1. Congo Red containing textile effluent benefits from the cooperative adsorption effect, which enhances removal efficiency even at moderate concentrations. However, the potential for dye aggregation should be considered in column design to prevent premature breakthrough.
2. Allura Red containing food industry wastewater can be effectively treated using activated carbon, with intraparticle diffusion as the rate-limiting step. This suggests that adsorbent particle size and pore structure are critical design parameters for optimizing AR removal.
3. Curcumin containing wastewater from food processing or pharmaceutical industries requires sufficient contact time due to the boundary layer-controlled chemisorption. Once adsorbed, CUR is strongly bound, minimizing desorption risks.

Table 3: Optimal conditions for wastewater treatment design

Dye	Optimal Conditions	Limitations	Recommendations
Congo Red, CR	pH 3–11, 0.5 g/50 mL, 30 min	None significant	Excellent candidate for CAC treatment; minimal optimization needed
Allura Red, AR	pH 3, 0.5 g/50 mL, >180 min	Low removal, pH sensitive, dosage sensitive	CAC unsuitable alone; require surface modification, alternative adsorbents, or combined processes
Curcumin, CUR	pH 3–7, 0.5 g/50 mL, 60 or >150 min	Complex kinetics, moderate removal	Treatable with CAC but require careful contact time optimization; avoid the 90-min dip

This study also shows that a single adsorbent (CAC) can effectively remove diverse dyes through different mechanisms, supporting its continued use as a versatile treatment medium.

Conclusion

This comprehensive kinetic and equilibrium study has showed the distinct adsorption mechanisms of three structurally different dyes (CR, AR and CUR) onto CAC. CR adsorption exhibited excellent fit to PSO model (R^2 = 0.9995) but conformed to the Freundlich isotherm (R^2 =

0.9960) with n = 0.91 (<1). This unique combination indicates chemisorption with cooperative effects. AR adsorption was best described by PFO model (R^2 = 0.9737) and the Freundlich isotherm (R^2 = 0.9915) with n = 1.31 (>1), indicating favourable physisorption onto a heterogeneous surface. CUR adsorption followed PSO model (R^2 = 0.9994) and the Langmuir isotherm (R^2 = 0.9972), indicating monolayer chemisorption onto a homogeneous surface. The Elovich model provided good fits for AR and CR, supporting the role of surface heterogeneity in their adsorption mechanisms, while the Temkin and linear models offered supplementary insights into adsorbate-adsorbent interactions.

The study also demonstrates that molecular structure profoundly influences adsorption mechanisms. The planar, highly aromatic structure of CR promotes cooperative adsorption; the polyphenolic nature of CUR drives specific chemical interactions; and the smaller, sulfonated structure of AR favours physical adsorption with intraparticle diffusion control.

These findings contribute to the fundamental understanding of dye-activated carbon interactions and provide a mechanistic basis for optimizing adsorption processes in wastewater treatment. It also highlight the importance of using multiple models and considering both kinetics and equilibrium data when elucidating adsorption mechanisms.

Future work will focus on: Thermodynamic studies to determine the spontaneity and energy changes associated with adsorption; column studies to evaluate practical applicability in continuous flow systems, and desorption and regeneration studies to assess adsorbent reusability and economic viability.

References

1. Crini, G. (2006). **Non-Conventional Low-Cost Adsorbents for Dye Removal:** A Review. *Bioresource Technology*, 97(9), 1061-1085.
2. Forgacs, E., Cserháti, T., and Oros, G. (2004). **Removal of Synthetic Dyes from Wastewaters:** A Review. *Environment International*, 30(7):953-971.
3. Gupta, V. K., and Suha, S. (2009). **Application of Low-Cost Adsorbents for Dye Removal:** A Review. *Journal of Environmental Management*, 90(8):2313-2342.
4. Chung, K. T. (2016). **Azo Dyes and Human Health:** A Review. *Journal of Environmental Science and Health, Part C*, 34(4):233-261.
5. Itodo A.U, Usman A., Grace A., Itodo H.U. and Ugboaja V.C (2012). **Performance Assessment of Received and Formulated Carbon Animalis: A Comparative Adsorption Isotherm Test.** *Journal of Environment Protection*. 3(3):288-295 **(**ISSN: 2152-2219) **By** Scientific Research Publishing**, China DOI: 10.4236/jep.2012.3303**
6. Purkait, M. K., Maiti, A., DasGupta, S., and De, S. (2007). **Removal of Congo Red Using Activated Carbon and its Regeneration.** *Journal of Hazardous Materials*, 145(1-2):287-295.
7. Rabia, R., Iqra, M. and Liviu, M. (2018). **Isothermal Study of Congo Red Dye Biosorptive Removal from Water by *Solanum Tuberosum* and *Pisum Sativum* Peels in Economical way.** *Bulletin of Chemical Society of Ethiopia,* 32(2):213-223, DOI: https://dx.doi.org/10.4314/bcse.v32i2.3
8. Vimonses, V., Lei, S., and Jin, B. (2009). **Kinetic Study and Equilibrium Isotherm Analysis of Congo Red Adsorption by Clay Materials.** *Chemical Engineering Journal*, 148(2-3):354-364.
9. Avila-Martínez, A.K., Roque-Ruiz, J.H., Torres-P´erez, J., Medellín-Castillo, N.A., ReyesLopez, S.Y. (2020). **Allura Red Dye Sorption onto Electrospun Zirconia Nanofibers.** *Environmental Technology and Innovation*. 18:100760-73 https://doi.org/10.1016/j.eti.2020.100760
10. Erdem, B., Erdem, M., and Özcan, A. S. (2016). **Adsorption of Reactive Black 5 and Allura Red AC from aqueous solutions by magnetic nanoparticles**. *Journal of the Turkish Chemical Society Section A: Chemistry*, 3(3):623-640.
11. Alkahtani, S.A., Abu-Alrub, S.S., Mahmoud, A.M., (2017). **Adsorption of Food Coloring Allura Red Dye (E129) from Aqueous Solutions using Activated Carbon.** *International Journal of Food Allied Science*, 3(10):110 - 126. https://doi.org/10.21620/ijfaas.2017110-26.
12. Bankole, D. T., Inyinbor, A. A., Oluyori, A. P., Arowolo, M. O. (2024). **Adsorptive Removal of Synthetic Food Dyes using Low-Cost Biochar: Efficiency Prediction, Kinetics and Desorption Index Evaluation.** *Bioresource Technology Reports,* 25:101709. https://doi.org/10.1016/j.biteb.2023.101709
13. Priyadarsini, K. I. (2014). **The Chemistry of Curcumin: From Extraction to Therapeutic Agent.** *Molecules*, 19(12):20091-20112.
14. Gholami, M., Vardini, M. T., and Mahdavinia, G. R. (2016). **Investigation of the Adsorption of Curcumin on the Functionalized Multi-Walled Carbon Nanotubes**. *Arabian Journal of Chemistry*, 9:S1635-S1642
15. Payal, A. and Behera, B. (2020). **Adsorption of Curcumin from Aqueous Solution using Different Adsorbents.** *Materials Today: Proceedings*, 29:1176-1181.
16. Chatterjee, S., Kumar, A., Basu, S. and Dutta, S. (2021). **Adsorption of Curcumin by Chitosan Hydrogel Beads.** *International Journal of Biological Macromolecules*, 181:1012-1021.
17. Verma, R.K., Sankhla, M.S., Rathod, N.V., Sonone, S.S., Parihar, K. and Singh, G.K. (2021). **Eradication of Fatal Textile Industrial Dyes by Wastewater Treatment.** *Biointerface Research Applied Chemistry*, 12(1):567-587.

18. Al Shamari, Y.M.G., Alwarthan, A.A., Wabaidur, S.M., Khan, M.A., Alqadami, A.A. and Siddiqui, M.R. (2020). **New Ultra Performance Liquid Chromatography-Mass Spectrometric Method for the Determination of Allura Red in Soft Drinks using Corncob as Solid Phase Extraction Sorbent: Analysis and Food Waste Management Approach.** *Journal of King Saudi University of Sciences,* 32:1135–1141. https://doi.org/10.1016/j.jksus.2019.10.011.

19. Moreno-Castilla, C. (2004). **Adsorption of Organic Molecules from Aqueous Solutions on Carbon Materials.** *Carbon*, 42(1):83-94.
20. Tan, I. A. W., Ahmad, A. L. and Hameed, B. H. (2008). **Adsorption of basic dye on high-surface-area activated carbon prepared from coconut husk.** *Journal of Hazardous Materials*, 154(1-3):337-346.

21. Allen, S. J., McKay, G. and Porter, J. F. (2004). **Adsorption Isotherm Models for Basic Dye Adsorption by Peat in Single and Binary Component Systems.** *Journal of Colloid and Interface Science*, 280(2):322-333.

22. Plazinski, W., Rudzinski, W. and Plazinska, A. (2009). **Theoretical Models of Sorption Kinetics Including a Surface Reaction Mechanism: A review.** *Advances in Colloid and Interface Science*, 152(1-2):2-13.

23. Azizian, S. (2004). **Kinetic Models of Sorption: A Theoretical Analysis.** *Journal of Colloid and Interface Science*, 276(1):47-52
24. Lagergren, S. (1898). **About the Theory of So-Called Adsorption of Soluble Substances.** *Kungliga Svenska Vetenskapsakademiens Handlingar*, 24(4):1-39.
25. Ho, Y. S. and McKay, G. (1999). **Pseudo-second Order Model for Sorption Processes.** *Process Biochemistry*, 34(5):451-465.

26. Simonin, J. P. (2016). **On the Comparison of Pseudo-First Order and Pseudo-Second Order Rate Laws in the Modeling of Adsorption Kinetics.** *Chemical Engineering Journal*, 300:254-263.
27. Largitte, L. and Pasquier, R. (2016). **A Review of the Kinetics Adsorption Models and their application to the Adsorption of lead by an Activated Carbon.** *Chemical Engineering Research and Design*, 109:495-504.

28. Low, M. J. D. (1960). **Kinetics of chemisorption of gases on solids.** *Chemical Reviews*, 60(3):267-312.
29. Weber, W. J. and Morris, J. C. (1963). **Kinetics of Adsorption on Carbon from Solution.** *Journal of the Sanitary Engineering Division*, 89(2):31-60.

30. Al-Ghouti, M. A. and Da'ana, D. A. (2020). **Guidelines for the use and interpretation of Adsorption Isotherm Models: A Review.** *Journal of Hazardous Materials*, 393:122383.
31. Foo, K. Y. and Hameed, B. H. (2010). **Insights into the Modeling of Adsorption Isotherm Systems.** *Chemical Engineering Journal*, 156(1):2-10.
32. Langmuir, I. (1918). **The Adsorption of Gases on Plane Surfaces of Glass, Mica and Platinum.** *Journal of the American Chemical Society*, 40(9):1361-1403.
33. Freundlich, H. (1906). **Over the Adsorption in Solution.** *Journal of Physical Chemistry*, 57(385), 1100-1107.
34. Itodo, A.U. and Itodo, H.U. (2011). **Application of Isotherm Studies on the Evaluation of Sorption Energies for Dyestuff Removal onto Derived Thermo-Cracked Shea Nut Shells.** *Electronic Journal of Environmental Agriculture and Food Chemistry* 10(3):1979-1987. University of Vigo, Spain. http://ejeafche.uvigo.es/component/option,com_docman/task,doc_view/gid,790/, 33/limit,20/limitstart,0/order,date/dir,DESC/(**ISSN:1579-4377)**

35. Temkin, M. I. and Pyzhev, V. (1940). **Kinetics of Ammonia Synthesis on Promoted Iron Catalysts.** *Acta Physiochimica URSS*, 12:327-356.

36. Wu, F. C., Tseng, R. L. and Juang, R. S. (2009). **Initial Behavior of Intraparticle diffusion model used in the description of Adsorption Kinetics**. *Chemical Engineering Journal*, 153(1-3):1-8.
37. Akande, J.A., Adeogun, A.I. and Uzosike, A.S. (2023). **Removal of Congo Red Dye from Simulated Wastewater Using Activated Carbon Derived from Corn Cobs; Kinetics and Equilibrium Studies.** *Global Journal of Pure and Applied Chemistry Research,* 11(1):1-19

38. Itodo, A.U. and Itodo, H.U. (2010). **Sorbents Capacities and Intensities of Thermochemically Cracked Shea nut Shells for the Removal of Wastewater Dyestuff**. *Academia arena* **2(**3-9):41-50. http://www.sciencepub.net/academia. **(ISSN: 1553-992X)**

39. Lorenc-Grabowska, E. and Gryglewicz, G. (2007). **Adsorption Characteristics of Congo Red on coal-based Mesoporous Activated Carbon.** *Dyes and Pigments*, 74(1):34-40.

40. Nandiyanto, A.B.D., Ragadhita, R., Fiandini, M. and Maryanti, R. (2023). **Curcumin Dye Adsorption in Aqueous Solution by Carbon Based Date Palm Seed: reparation, Characterization, and Isotherm Adsorption.** *Journal of Applied Research and Technology,* (21):808-824.

41. Dawood, S. and Sen, T. K. (2012). **Removal of Anionic Dye Congo Red from Aqueous Solution by Raw Pine and Acid-Treated**

Pine Cone Powder as Adsorbent. *Water Research*, 46(6):1933-1946.

42. Ghzal, Q., Javed, T. and Batool, M. (2023). **Potential of Easily Prepared Low-Cost Rice Husk Biochar and Burnt Clay Composite for Removal of Methylene Blue Dye from Contaminated Water.** *Environmental Science: Water Research and Technology,* 9:2925–2941.
43. Thompson, M. and Ellison, S. L. (2011). **A Review of Interference Effects and their Correction in Chemical Analysis with Special Reference to uncertainty.** *Accreditation and Quality Assurance*, 16:285-291.
44. Salleh, M. A. M., Mahmoud, D. K., Karim, W. A. W. A. and Idris, A. (2011). **Cationic and Anionic Dye Adsorption by Agricultural Solid Wastes: A Comprehensive Review.** *Desalination*, 280(1-3):1-13.
45. McKay, G. (1983). **The Adsorption of Dyestuffs from Aqueous Solutions using Activated Carbon: Analytical Solution for Batch Adsorption.** *Journal of Chemical Technology and Biotechnology*, 33(4):196-204.
46. Sircar, S. and Rao, M. B. (1999). **Kinetic and Isotherm Analysis of Surfactant Adsorption.** *AIChE Journal*, 45(4):805-815.
47. Wang, Y. J., Pan, M. H. and Cheng, A. L. (1997). **Stability of Curcumin in Buffer Solutions and Characterization of Its Degradation Products.** *Journal of Pharmaceutical and Biomedical Analysis*, 15(12):1867-1876.
48. Rudzinski, W. and Plazinski, W. (2007). **Theoretical Description of the Kinetics of Solute Adsorption at Heterogeneous Solid/Solution Interfaces.** *Applied Surface Science*, 253(13):5827-5840.
49. Oladoye, P. O., Bamigboye, M. O., Ogunbiyi, O. D. and Akano, M. T. (2022) **Toxicity and Decontamination Strategies of Congo Red Dye.** *Groundwater for Sustainable Development,* 19:100844.
50. Sips, R. (1948). **On the Structure of a Catalyst Surface.** *The Journal of Chemical Physics*, 16(5):490-495.
51. Chen, W., Duan, L. and Zhu, D. (2007). **Adsorption of Polar and Nonpolar Organic Chemicals to Carbon Nanotubes.** *Environmental Science and Technology*, 41(24):8295-8300.

Cite this article

Itodo H.U., Asema M.A., & Apochi J.O. (2026). Structure-Dependent Adsorption of Synthetic and Natural Dyes onto Commercial Activated Carbon: Kinetic, Diffusion, and Isotherm Modelling. FUAM Journal of Pure and Applied Science, **6**(**2**):91-105